Level Set Method for Shape and Topology Optimization in Elasticity

Shape Gradients and Topological Derivatives

Yixin Tan

East China Normal University
Systems Research Institute of the Polish Academy of Sciences

Joint work with Prof. Jan Sokolowski

Meeting of the Optimization Section Committee on Mechanics, Polish Academy of Sciences

Outline

Background

- Engineering Demand
  - Lightweight design is not only related to material costs and transportation efficiency, but also a core approach to improving energy efficiency and reducing carbon emissions. In the aerospace industry, every $1kg$ reduction in structural weight can save approximately $100,000US$ dollars in the full life-cycle cost. In the automotive industry, a 10% decrease in vehicle body weight leads to a 6–8% improvement in fuel efficiency. This makes efficient structural optimization technology the "core engine" of modern high-end manufacturing.
- Core Technology
  - Structural optimization techniques are mainly classified into three categories: sizing optimization, shape optimization, and topology optimization. Sizing optimization adjusts component parameters; shape optimization smoothes boundaries under a fixed topology; while topology optimization can freely explore the optimal material distribution and connectivity within the design space, making it the most powerful tool for creating novel structural configurations. This study focuses on a hybrid strategy combining shape and topology optimization.

Motivation

- Limitations of Traditional Methods
  - Sizing and shape optimization: Heavily dependent on the initial design, unable to break through the limitations of inherent topology, and prone to falling into local optimal solutions.
  - Density method (SIMP): Often accompanied by numerical drawbacks such as checkerboarding and mesh dependency, with blurred boundaries in the optimization results.
  - Traditional level-set method: Generally requires predefined initial holes to achieve topological changes, and volume control is relatively difficult.
- Our Research Goal
  - To construct a highly efficient, stable and robust structural optimization framework. By integrating shape gradients and topological derivatives, we achieve topological innovation (automatic discovery of optimal load paths), smooth boundaries (ready for direct manufacturing), and stable high efficiency with implicit volume control.

Key Contributions of This Work

- Novel Hybrid Strategy
  - Proposes a hybrid optimization framework merging shape gradients (implemented through gradient flow) with topological derivatives.
- Implicit Volume Control
  - Uses boundary energy density penalization instead of explicit constraints for stability.
- Efficient Sensitivity Calculation
  - Simplifies derivative calculations using the adjoint method for computational efficiency.
- Comprehensive Validation
  - Validates effectiveness through thorough 2D and 3D numerical examples.

Contents

Model problem

- Strong Form Equations
  - Equilibrium: $\nabla \cdot \sigma + f = 0$ in Ω
    - It describes the equilibrium relationship between the divergence of stress and body forces on a differential element, serving as the foundation of structural static analysis.
  - Constitutive: $\sigma = C\varepsilon(u)$
    - Known as the generalized Hooke's law, it establishes a linear relationship between stress and strain, where C denotes the fourth-order elasticity tensor.
  - Kinematic: $\varepsilon(u) = \left(\nabla u + \nabla u^T\right)/2$
    - The geometric relationship between the strain tensor and the displacement vector under the small deformation assumption is defined, which relates the rate of change of the displacement field to the strain.

Model problem

- Boundary Conditions
  - Dirichlet: $u = 0$ on Γ_D
  - Neumann: $\sigma(u) \cdot n = g$ on Γ_N
  - Free Boundary: $\sigma(u) \cdot n = 0$ on Γ

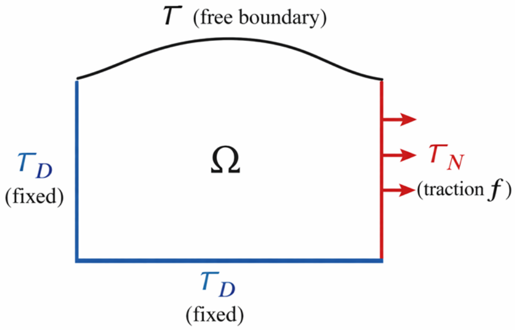

Optimization Objective

- Our objective is to improve the structural stiffness, which is commonly measured by the compliance-type functional
$$\mathcal{J}(\Omega) = \int_{\Gamma_N} \mathbf{g} \cdot \mathbf{u} \, ds, \tag{1}$$
where $\mathbf{g}$ is the applied load on Γ_N and $\mathbf{u}$ is the resulting displacement of the elastic body.
- Minimizing $\mathcal{J}(\Omega)$ corresponds to reducing the deformation under the applied load and hence improving stiffness. However, this condition provides only necessary optimality and is not locally sufficient; in fact, without additional regularization or descent control, the procedure may even lead to an increase of compliance in certain configurations. This limitation is addressed by the penalization and stabilization mechanisms introduced in the sequel.

- The optimization problem involves minimizing a functional subject to constraints on the domain. The Lagrangian for this problem is formulated as:

$$L(\Omega, \mu) = \int_{\Gamma_N} \mathbf{g} \cdot \mathbf{u} \, ds + \mu \left[\int_{\Omega} dx - V_0 \right], \tag{2}$$

  where the first term represents the mechanical work on the boundary Γ_N due to the applied force $\mathbf{g}$, and the second term enforces the volume constraint $\int_{\Omega} dx \leq V_0$. Here, μ denotes a value of the energy density.

- By differentiating the Lagrangian and the state equation with respect to the shape, we obtain the optimality condition:

$$\boldsymbol{\sigma}(\mathbf{u}) : \boldsymbol{\varepsilon}(\mathbf{u}) = \mu \quad \text{on } \Gamma. \tag{3}$$

  The condition states that the (twice) strain-energy density is uniform along Γ at optimality.

Contents

Definition

Definition

Let $\Omega \subset \mathbb{R}^d$ be a domain, and let $J(\Omega)$ be a shape functional defined on a class of admissible domains. Consider a smooth vector field $\mathcal{V} : \mathbb{R}^d \to \mathbb{R}^d$ and the associated perturbation of Ω given by the transformation

$$T_t(x) = x + t\mathcal{V}(x), \quad t \in [0, \varepsilon]$$

The perturbed domain is $\Omega_t = T_t(\Omega)$. The shape derivative of J at Ω in the direction $\mathcal{V}$ is defined as

$$dJ(\Omega)[\mathcal{V}] = \lim_{t \to 0^+} \frac{J(\Omega_t) - J(\Omega)}{t}$$

whenever the above limit exists. We also denote this form of shape derivative as $J'(\Omega)$.

It measures the first-order variation of the objective functional induced by a geometric perturbation of the domain and forms the foundation of gradient-based shape optimization methods.

If $\mathbf{u}_t(\mathbf{x})$ denotes a state variable (scalar or vector) defined on the perturbed domain Ω_t, then its shape derivative at Ω_0 in the direction of $\mathcal{V}$ is given by

$$\mathbf{u}_0'(\mathbf{x}) = \lim_{t\to 0^+} \frac{\mathbf{u}_t(\mathbf{x}) - \mathbf{u}_0(\mathbf{x})}{t}. \tag{4}$$

This derivative quantifies the first-order variation of $\mathbf{u}_t$ due to domain deformations and provides the foundation for deriving sensitivity formulas of functionals depending on Ω.

Equivalent Form

The following penalized functional has been introduced in earlier works. This formulation is integrated into the present computational framework, and its numerical performance is analyzed. To address the optimization problem, the functional is reformulated to penalize deviations of the mechanical energy density from a target value μ. Specifically, the objective functional is defined as

$$\mathcal{J}(\Omega) = \int_{\Gamma_v} G\big(\boldsymbol{\sigma}(\mathbf{u}) : \boldsymbol{\varepsilon}(\mathbf{u}) - \mu\big)\, ds, \tag{5}$$

where the function $G(a)$ is carefully chosen to apply penalties only outside a certain tolerance interval around zero.

In the present context, this functional provides a mechanism to balance penalization and stability, and its influence on convergence properties will be illustrated in the numerical experiments. Here, $\Gamma_v \subset \partial\Omega$ denotes the variable (design) part of the boundary on which the penalty functional is imposed. This is achieved by defining $G(a)$ as:

$$G(a) = \begin{cases} (a+b)^2 & a < -b, \\ 0 & -b \leq a \leq b, \\ (a-b)^2 & a > b, \end{cases} \tag{6}$$

where $b > 0$ specifies the tolerance interval. After computing a, the value of b is adapted to a following the rule $b = a/4$. This construction ensures that deviations within $[-b, b]$ are ignored, while quadratic penalties are applied to values outside this range.

Related Formulations

The shape derivative of $J(\Omega)$ is then obtained as:

$$\begin{aligned} J'(\Omega) = 2\int_{\Gamma_v} G'\left(\boldsymbol{\sigma}(\mathbf{u}) : \boldsymbol{\varepsilon}(\mathbf{u}) - \mu\right)\left(\boldsymbol{\sigma}(\mathbf{u}') : \boldsymbol{\varepsilon}(\mathbf{u})\right) ds \\ + \int_{\Gamma_v} \left(\frac{\partial G}{\partial n} + \kappa G\right)(\mathcal{V} \cdot \mathbf{n})\, ds, \end{aligned} \tag{7}$$

where κ is the mean curvature of the boundary Γ_v, and the term $\frac{\partial G}{\partial n}$ accounts for normal variations of G:

$$\frac{\partial G}{\partial n} = G'\left(\boldsymbol{\sigma}(\mathbf{u}) : \boldsymbol{\varepsilon}(\mathbf{u}) - \mu\right)\frac{\partial}{\partial n}\left(\boldsymbol{\sigma}(\mathbf{u}) : \boldsymbol{\varepsilon}(\mathbf{u})\right). \tag{8}$$

To eliminate the explicit dependence on $\mathbf{u}'$, an adjoint problem is introduced. The adjoint variable $\mathbf{p}$ satisfies the following weak form:

$$\int_\Omega \boldsymbol{\sigma}(\mathbf{p}) : \boldsymbol{\varepsilon}(\mathbf{v})\, dx + \int_{\Gamma_v} G'\big(\boldsymbol{\sigma}(\mathbf{u}) : \boldsymbol{\varepsilon}(\mathbf{u}) - \mu\big) \big(\boldsymbol{\sigma}(\mathbf{u}) : \boldsymbol{\varepsilon}(\mathbf{v})\big)\, ds = 0, \tag{9}$$

where $\mathbf{p}$ and $\mathbf{v}$ are both test functions in the Sobolev space $\mathbf{H}^1_{\Gamma_D}(\Omega)$. In the algorithm, this equation is solved using the finite element method.

The adjoint problem enables the elimination of $\mathbf{u}'$ in the shape derivative. By choosing $\mathbf{v} = \mathbf{p}$ in the shape-differentiated state equation and $\mathbf{v} = \mathbf{u}'$ in the adjoint equation, the integral involving $\mathbf{u}'$ can be transformed. This gives:

$$\int_{\Gamma_v} G'\big(\boldsymbol{\sigma}(\mathbf{u}) : \boldsymbol{\varepsilon}(\mathbf{u}) - \mu\big) \big(\boldsymbol{\sigma}(\mathbf{u}) : \boldsymbol{\varepsilon}(\mathbf{u}')\big)\, ds = \int_{\Gamma_v} \big(\boldsymbol{\sigma}(\mathbf{u}) : \boldsymbol{\varepsilon}(\mathbf{p})\big)(\mathcal{V} \cdot \mathbf{n})\, ds. \tag{10}$$

Finally, substituting this result into the shape derivative of the functional yields:

$$J'(\Omega) = \int_{\Gamma_v} \left(2\big(\boldsymbol{\sigma}(\mathbf{u}) : \boldsymbol{\varepsilon}(\mathbf{p})\big) + \frac{\partial G}{\partial n} + \kappa G\right)(\mathcal{V} \cdot \mathbf{n})\, ds. \tag{11}$$

Normalization

A direct tendency to minimize the area of the variable boundary Γ_v may lead to undesirable degeneracies in the optimization process. Since the objective is only to enforce a constant energy density along Γ_v, it is more appropriate to normalize the functional by the boundary measure. In this way, the modified functional is defined as

$$\tilde{J}(\Omega) = \frac{J(\Omega)}{\int_{\Gamma_v} ds} = \frac{\int_{\Gamma_v} G(\boldsymbol{\sigma}(\mathbf{u}) : \varepsilon(\mathbf{u}) - \mu)\, ds}{\int_{\Gamma_v} ds}. \tag{12}$$

Its shape derivative follows from the quotient rule together with the same adjoint system used for J. Then we obtain

$$\tilde{J}'(\Omega) = \frac{1}{|\Gamma_v|} \int_{\Gamma_v} \left(2\boldsymbol{\sigma}(\mathbf{u}) : \boldsymbol{\varepsilon}(\mathbf{p}) + \frac{\partial G}{\partial n} + \kappa(G - \bar{G}) \right) \mathcal{V} \cdot \mathbf{n}\, ds, \tag{13}$$

where $\mathbf{p}$ is the adjoint state that eliminates the material derivative of $\mathbf{u}$ and $|\Gamma_v| = \int_{\Gamma_v} ds$.

Contents

Topology perturbation

Domain decomposition techniques, combined with the Steklov–Poincaré pseudo-differential boundary operator, are commonly employed in topological asymptotic analysis for the nucleation of small circular inclusions. Consider an open and bounded domain $\Omega \subset \mathbb{R}^d$ $(d = 2, 3)$, subject to a nonsmooth perturbation confined to a small region $\omega_\varepsilon(\widehat{x}) = \widehat{x} + \varepsilon\omega$ of size ε, with $\overline{\omega_\varepsilon} \Subset \Omega$, as shown in Fig. 2. Here, $\widehat{x}$ is an arbitrary point in Ω and ω is a fixed domain in $\mathbb{R}^d$.

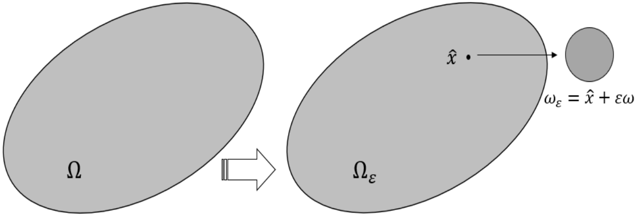

Figure: Illustration of the topological derivative.

Define the singular perturbation of Ω as $\Omega_\varepsilon := \Omega\backslash\overline{\omega_\varepsilon}$. Consider the state equation and the adjoint state equation in the perturbed domain Ω_ε:

$$\int_{\Omega_\varepsilon} \boldsymbol{\sigma}\left(\mathbf{u}_\varepsilon\right) : \boldsymbol{\varepsilon}(\boldsymbol{\varphi})\, dx = \int_{\Gamma_N} \mathbf{g}\cdot\boldsymbol{\varphi}\, ds \quad \forall\boldsymbol{\varphi}\in\mathbf{V}(\Omega_\varepsilon), \tag{14}$$

$$\int_{\Omega_\varepsilon} \boldsymbol{\sigma}(\mathbf{p}_\varepsilon) : \boldsymbol{\varepsilon}(\boldsymbol{\varphi})\, dx + \int_{\Gamma_v} G'\big(\boldsymbol{\sigma}(\mathbf{u}_\varepsilon) : \boldsymbol{\varepsilon}(\mathbf{u}_\varepsilon) - \mu\big)\, \boldsymbol{\sigma}(\mathbf{u}_\varepsilon) : \boldsymbol{\varepsilon}(\boldsymbol{\varphi})\, ds = 0 \quad \forall\boldsymbol{\varphi}\in\mathbf{V}(\Omega_\varepsilon). \tag{15}$$

Here and throughout, the symbol $\boldsymbol{\varphi}$ denotes a generic test function; the state $\mathbf{u}_\varepsilon$ and adjoint $\mathbf{p}_\varepsilon$ are the unique solutions of (14)–(15).

The shape functional in Ω_ε is

$$J_\mu(\Omega_\varepsilon) = \int_{\Gamma_v} G\big(\boldsymbol{\sigma}(\mathbf{u}_\varepsilon) : \boldsymbol{\varepsilon}(\mathbf{u}_\varepsilon) - \mu\big)\, ds. \tag{16}$$

Now decompose Ω_ε into two parts, namely $\Omega_\varepsilon = \Omega_R \cup \overline{C(R,\varepsilon)}$, where $\Omega_R := \Omega_\varepsilon\backslash\overline{C(R,\varepsilon)}$ and $C(R,\varepsilon)$ (with outer boundary Γ_R) denotes a ball of radius $R>0$ centered at an arbitrary point $\widehat{x}\in\Omega$, containing the hole ω_ε inside $C(R,\varepsilon)$ with $R \gg \varepsilon > 0$.

Topological derivative

We identify the family of Steklov–Poincaré boundary operators on the outer boundary Γ_R of the domain $C(R, \varepsilon)$. For the boundary value problem defined in Ω_ε, we introduce a truncated problem within Ω_R. The singular perturbation Ω_ε of the geometrical domain Ω is thus replaced by a regular perturbation of the Steklov–Poincaré boundary operator defined on the interface, which coincides with the interior boundary Γ_R of Ω_R.

Definition

The Steklov–Poincaré boundary operator

$$\mathcal{S}_\varepsilon : H^{1/2}(\Gamma_R) \to H^{-1/2}(\Gamma_R) \tag{17}$$

is defined for the elasticity equation in the domain $C(R, \varepsilon)$.

For a fixed parameter $\varepsilon > 0$ and a given element $\mathbf{v} \in H^{1/2}(\Gamma_R)$, the corresponding element in the range of the operator $\mathcal{S}_\varepsilon$ is given by the Neumann trace of a unique solution to the boundary value problem

$$\text{Find } \mathbf{w}_\varepsilon \text{ such that } \begin{cases} -\operatorname{div}(\boldsymbol{\sigma}(\mathbf{w}_\varepsilon)) = 0 & \text{in } C(R,\varepsilon), \\ \mathbf{w}_\varepsilon = \mathbf{v} & \text{on } \Gamma_R, \\ \boldsymbol{\sigma}(\mathbf{w}_\varepsilon)\cdot\mathbf{n} = 0 & \text{on } \partial\,\omega_\varepsilon. \end{cases} \tag{18}$$

Then we set

$$\mathcal{S}_\varepsilon(\mathbf{v}) = \boldsymbol{\sigma}(\mathbf{w}_\varepsilon)\cdot\boldsymbol{\nu} \quad \text{on} \quad \Gamma_R, \tag{19}$$

where $\boldsymbol{\nu}$ is the unit exterior normal vector on $\partial C(R,\varepsilon)$ and $\boldsymbol{\nu} = -\mathbf{n}$. If $\mathbf{v} = \mathbf{u}_{\varepsilon|\Gamma_R}$, then $\mathbf{w}_\varepsilon = \mathbf{u}_{\varepsilon|C(R,\varepsilon)}$ and $\mathbf{u}_\varepsilon^R = \mathbf{u}_{\varepsilon|\Omega_R}$, where $\mathbf{u}_\varepsilon$ is the solution of the perturbed problem in Ω_ε.

By definition of $\mathcal{S}_\varepsilon$, the solution $\mathbf{w}_\varepsilon$ of (18) satisfies:

$$\int_{C(R,\varepsilon)} \boldsymbol{\sigma}(\mathbf{w}_\varepsilon) : \boldsymbol{\varepsilon}(\mathbf{w}_\varepsilon)\, dx = \int_{\Gamma_R} \mathcal{S}_\varepsilon(\mathbf{w}_\varepsilon) \cdot \mathbf{w}_\varepsilon\, ds. \tag{20}$$

The Steklov–Poincaré operator for the ring $C(R,\varepsilon)$ admits, for sufficiently small $\varepsilon > 0$, the expansion

$$\mathcal{S}_\varepsilon = \mathcal{S} + \varepsilon^d \mathcal{S}_1 + \mathcal{R}_\varepsilon, \tag{21}$$

where the remainder $\mathcal{R}_\varepsilon$ is of order $o(\varepsilon^d)$ in the operator norm $\mathcal{L}\big(H^{1/2}(\Gamma_R); H^{-1/2}(\Gamma_R)\big)$.

Consider the state equation in Ω_R with $\mathcal{S}_\varepsilon$: find $\mathbf{u}_\varepsilon^R \in \mathbf{V}(\Omega_R)$ such that $\forall \boldsymbol{\varphi} \in \mathbf{V}(\Omega_R)$,

$$\int_{\Omega_R} \boldsymbol{\sigma}(\mathbf{u}_\varepsilon^R) : \boldsymbol{\varepsilon}(\boldsymbol{\varphi})\, dx + \langle \mathcal{S}_\varepsilon(\mathbf{u}_\varepsilon^R), \boldsymbol{\varphi}\rangle_{\Gamma_R} = \langle \mathbf{g}_\varepsilon^R, \boldsymbol{\varphi}\rangle_{\Gamma_N}, \tag{22}$$

and set

$$a(\Omega_R; \mathbf{u}_\varepsilon^R, \boldsymbol{\varphi}) := \int_{\Omega_R} \boldsymbol{\sigma}(\mathbf{u}_\varepsilon^R) : \boldsymbol{\varepsilon}(\boldsymbol{\varphi})\, dx.$$

Similarly, the adjoint equation in Ω_R with $\mathcal{S}_\varepsilon$ is: find $\mathbf{p}_\varepsilon^R \in \mathbf{V}(\Omega_R)$ such that $\forall \boldsymbol{\varphi} \in \mathbf{V}(\Omega_R)$,

$$\int_{\Omega_R} \boldsymbol{\sigma}(\mathbf{p}_\varepsilon^R) : \boldsymbol{\varepsilon}(\boldsymbol{\varphi})\, dx + \langle \mathcal{S}_\varepsilon(\mathbf{p}_\varepsilon^R), \boldsymbol{\varphi}\rangle_{\Gamma_R} = -\int_{\Gamma_v} G'\big(\boldsymbol{\sigma}(\mathbf{u}_\varepsilon^R) : \boldsymbol{\varepsilon}(\mathbf{u}_\varepsilon^R) - \mu\big)\, \boldsymbol{\sigma}(\mathbf{u}_\varepsilon^R) : \boldsymbol{\varepsilon}(\boldsymbol{\varphi})\, ds. \tag{23}$$

By Green's formula, we obtain

$$a\big(C(R,\varepsilon);\mathbf{w}_\varepsilon,\mathbf{w}_\varepsilon\big) = \langle \mathcal{S}_\varepsilon(\mathbf{w}_\varepsilon),\mathbf{w}_\varepsilon\rangle_{\Gamma_R} = -\langle \mathcal{S}_\varepsilon(\mathbf{u}_\varepsilon^R),\mathbf{u}_\varepsilon^R\rangle_{\Gamma_R}, \tag{24}$$

where the minus sign follows from traction continuity across Γ_R and the opposite orientation of the unit normals on the two sides ($\boldsymbol{\nu} = -\mathbf{n}$). Thus $\mathcal{S}_\varepsilon(\mathbf{w}_\varepsilon) = -\,\mathcal{S}_\varepsilon(\mathbf{u}_\varepsilon^R)$ on Γ_R.
It is well known that the topological asymptotic expansion of the energy functional takes the form :

$$\int_{C(R,\varepsilon)} \boldsymbol{\sigma}\,(\boldsymbol{\varphi}) : \boldsymbol{\varepsilon}(\boldsymbol{\varphi})\,dx = \int_{B_R} \boldsymbol{\sigma}(\boldsymbol{\varphi}) : \boldsymbol{\varepsilon}(\boldsymbol{\varphi})\,dx + \varepsilon^d\,\mathbb{P}_\gamma : \big(\boldsymbol{\sigma}(\boldsymbol{\varphi}) \otimes \boldsymbol{\varepsilon}(\boldsymbol{\varphi})\big) + o(\varepsilon^d), \tag{25}$$

where we emphasize that $\boldsymbol{\varphi} = \mathbf{u}|_{B_R}$ denotes the restriction of the *unperturbed state* $\mathbf{u}$ to B_R (and not a generic test function).

According to (21) and the symmetry of the Steklov–Poincaré operator, the expansion of the boundary form can be written as

$$\langle \mathcal{S}_\varepsilon(\boldsymbol{\varphi}), \boldsymbol{\vartheta}\rangle = \langle \mathcal{S}(\boldsymbol{\varphi}), \boldsymbol{\vartheta}\rangle + \varepsilon^d \langle \mathcal{S}_1(\boldsymbol{\varphi}), \boldsymbol{\vartheta}\rangle + \langle \mathcal{R}_\varepsilon(\boldsymbol{\varphi}), \boldsymbol{\vartheta}\rangle \,, \tag{26}$$

where $\langle \mathcal{R}_\varepsilon(\boldsymbol{\varphi}), \boldsymbol{\vartheta}\rangle = o(\varepsilon^d)$.
Then, the topological derivative of the energy in $C(R,\varepsilon) \subset \mathbb{R}^d$ is

$$a(C(R,\varepsilon); \boldsymbol{\varphi}_\varepsilon, \boldsymbol{\varphi}_\varepsilon) = a(B_R; \boldsymbol{\varphi}, \boldsymbol{\varphi}) + \varepsilon^d \langle \mathbb{P}_\gamma \boldsymbol{\sigma}(\boldsymbol{\varphi}), \boldsymbol{\varepsilon}(\boldsymbol{\varphi})\rangle + o(\varepsilon^d). \tag{27}$$

From (24), we obtain

$$-\langle \mathcal{S}_\varepsilon(\mathbf{u}_\varepsilon^R), \mathbf{u}_\varepsilon^R\rangle_{\Gamma_R} = a(B_R; \mathbf{u}|_{B_R}, \mathbf{u}|_{B_R}) + \varepsilon^d \langle \mathbb{P}_\gamma \boldsymbol{\sigma}(\mathbf{u}|_{B_R}), \boldsymbol{\varepsilon}(\mathbf{u}|_{B_R})\rangle + o(\varepsilon^d). \tag{28}$$

Thus, we obtain

$$\langle \mathcal{S}_1(\boldsymbol{\varphi}), \boldsymbol{\vartheta} \rangle = -\mathbb{P}_\gamma \boldsymbol{\sigma}(\boldsymbol{\varphi}(\widehat{x})) : \boldsymbol{\varepsilon}(\boldsymbol{\vartheta}(\widehat{x})) \quad \forall \widehat{x} \in \Omega. \tag{29}$$

We consider the following ansatz for the solutions $\mathbf{u}_\varepsilon, \mathbf{p}_\varepsilon$:

$$\mathbf{u}_\varepsilon = \mathbf{u} + \varepsilon^d \mathbf{u}_1 + \widetilde{\mathbf{u}}_\varepsilon, \qquad \mathbf{p}_\varepsilon = \mathbf{p} + \varepsilon^d \mathbf{p}_1 + \widetilde{\mathbf{p}}_\varepsilon, \tag{30}$$

where $\mathbf{u}, \mathbf{p}$ solve (14), (15); $\mathbf{u}_1, \mathbf{p}_1$ are the first-order correction terms, and $\widetilde{\mathbf{u}}_\varepsilon, \widetilde{\mathbf{p}}_\varepsilon$ are the remainders.
Differentiating (22) with $\rho = \varepsilon^d$ at $\varepsilon = 0^+$ gives

$$a(\Omega_R; \mathbf{u}_1, \boldsymbol{\varphi}) + \langle \mathcal{S}(\mathbf{u}_1), \boldsymbol{\varphi} \rangle_{\Gamma_R} + \langle \mathcal{S}_1(\mathbf{u}), \boldsymbol{\varphi} \rangle_{\Gamma_R} = 0. \tag{31}$$

For the unperturbed adjoint problem on Ω_R we equivalently write

$$\int_{\Omega_R} \boldsymbol{\sigma}(\mathbf{p}) : \boldsymbol{\varepsilon}(\boldsymbol{\varphi})\, dx + \langle \mathcal{S}(\mathbf{p}), \boldsymbol{\varphi} \rangle_{\Gamma_R} = -\int_{\Gamma_v} G'\big(\boldsymbol{\sigma}(\mathbf{u}) : \boldsymbol{\varepsilon}(\mathbf{u}) - \mu\big)\, \boldsymbol{\sigma}(\mathbf{u}) : \boldsymbol{\varepsilon}(\boldsymbol{\varphi})\, ds. \tag{32}$$

By taking $\mathbf{u}_1$ as a test function in (32) and $\mathbf{p}$ as a test function in (31), we obtain

$$\int_{\Gamma_v} G'\big(\boldsymbol{\sigma}(\mathbf{u}) : \boldsymbol{\varepsilon}(\mathbf{u}) - \mu\big)\, \boldsymbol{\sigma}(\mathbf{u}) : \boldsymbol{\varepsilon}(\mathbf{u}_1)\, ds = \int_{\Gamma_R} \mathcal{S}_1(\mathbf{u}) \cdot \mathbf{p}\, ds = -\mathbb{P}_\gamma \boldsymbol{\sigma}(\mathbf{u}) : \boldsymbol{\varepsilon}(\mathbf{p}). \tag{33}$$

Hence, the topological derivative is

$$\mathcal{T}(\hat{x}) = -2\, \mathbb{P}_\gamma \boldsymbol{\sigma}(\mathbf{u}(\hat{x})) : \boldsymbol{\varepsilon}(\mathbf{p}(\hat{x})). \tag{34}$$

Here, $\mathbb{P}_\gamma$ is a fourth-order isotropic polarization tensor:

$$\mathbb{P}_\gamma = \frac{1}{4} \frac{(1-\gamma)^2}{1+\beta\gamma} \left(2 \frac{1+\beta}{1-\gamma} \mathbb{I} + \frac{\alpha-\beta}{1+\alpha\gamma} \mathrm{I} \otimes \mathrm{I} \right), \tag{35}$$

where $\mathbb{I}$ is the fourth-order identity, I the second-order identity, and the parameters α and β are given by

$$\alpha = \frac{1+\nu}{1-\nu}, \qquad \beta = \frac{3-\nu}{1+\nu},$$

with ν being Poisson's ratio, and $\gamma \in [0, \infty)$ the contrast.

Contents

Level set function

We describe the domain using a level set function as follows:

$$\begin{cases} \phi(x) < 0 & \forall x \in \Omega, \\ \phi(x) = 0 & \forall x \in \Gamma, \\ \phi(x) > 0 & \forall x \in D \backslash \Omega, \end{cases}$$

where D denotes the design domain, i.e., the computational domain of the problem; Ω is the current domain; and Γ is the boundary of Ω.

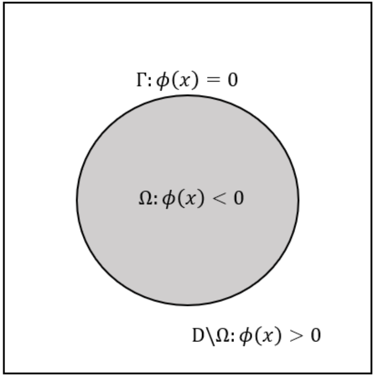

Figure: Schematic design domain with the level set function

Geometric Quantities

The unit normal to $\partial\Omega$ is

$$n = \frac{\nabla\phi}{|\nabla\phi|}. \tag{36}$$

We also introduce the Heaviside function and the Dirac delta function, defined by

$$H(x) = \begin{cases} 1, & \text{if } x \geqslant 0 \\ 0, & \text{otherwise} \end{cases} \tag{37}$$

and

$$\delta(\cdot - 0) \in \mathcal{D}'(R), \tag{38}$$

where $\mathcal{D}'(R)$ denotes the space of distributions. Then,

$$|\Omega| = \int_D (1 - H(\phi))\, dx \quad \text{and} \quad |\partial\Omega| = \int_\Gamma ds = \int_D \delta(\phi(x))\, |\nabla\phi(x)|\, dx.$$

Shape gradient with the level set function

To increase smoothness and extend the velocity at the interface to the entire domain where the level set equation is defined, we introduce the H^1-gradient flow: find $\theta \in [H^1(D)]^2$ such that $\forall \mathcal{V} \in [H^1(D)]^2$

$$\int_D \omega \mathrm{D}\theta : \mathrm{D}\mathcal{V} + \theta \cdot \mathcal{V} \, d\mathbf{x} = -\tilde{J}'(\Omega)(\mathcal{V}), \tag{39}$$

where $\omega > 0$ is a diffusion parameter.

$$\begin{cases} \phi_t + \theta \cdot \nabla \phi = 0 & \text{in } U, \\ \phi(0, x) = \phi_0(x) & \text{in } D, \end{cases} \tag{40}$$

where $U := D \times \mathbb{R}^+$, θ is the velocity field, and ϕ_0 is the initial level set function.

On $\Gamma(t)$ one has $\theta \cdot \mathbf{n} = V_n$ (the normal velocity). Extending V_n off the interface yields the familiar form $\phi_t + V_n |\nabla \phi| = 0$, which shows that the apparent interface speed scales with $|\nabla \phi|$. To solve this convection problem, we employ the characteristic Galerkin finite element method. As the domain evolves, the level set function may become too steep or too flat, leading to numerical instabilities, degrading the accuracy of geometric quantities (normals and curvature) and introducing spurious scaling in the advection. An idealized situation corresponds to the case $|\nabla \phi| = 1$, which characterizes ϕ as a signed distance function.
This property is fundamental in level-set methods, since it guarantees that the level-set function evolves without excessive distortion and preserves a uniform gradient magnitude near the interface.
In practice, this condition is often enforced through reinitialization techniques to maintain numerical stability.

Shape evolution equation

This condition is achieved (or approximately enforced) using a signed distance function, defined as

$$\phi(x) = \begin{cases} \varphi(x;\Gamma) & \text{in } \Omega, \\ 0 & \text{on } \Gamma, \\ -\varphi(x;\Gamma) & \text{in } D\backslash\Omega, \end{cases} \tag{41}$$

where $\varphi(x;\Gamma) := \min_{y\in\Gamma} |x-y|$ represents the shortest distance from x to the boundary Γ. In practice one enforces $|\nabla\phi| \approx 1$ in a narrow band around Γ. To maintain the regularity of the level set function, a "reinitialization" procedure is commonly applied. This involves solving the following nonlinear equation for $\phi = \phi(t,x)$, evolving it until it reaches a steady state:

$$\begin{cases} \psi_\tau + \operatorname{sign}(\phi)\left(|\nabla\psi| - 1\right) = 0 \quad \text{in } U, \\ \psi(0,x) = \phi(t,x) \text{ in } D, \end{cases} \tag{42}$$

Contents

Algorithm 1: Shape gradient method for optimization.

Input: Initial level-set function ϕ_0, initial step size t_0, maximum number of iterations $n_{\max} \in \mathbb{N}$, multiplier μ, perform reinitialization every k steps.

for $n = 0, 1, 2, \ldots, n_{max}$ **do**
- Solve the state equation (7) and the adjoint state equation (17);
- Compute the shape gradient $\tilde{J}_\mu(\Omega_n)'$;
- Solve the H^1-gradient flow (50) to obtain θ_n;
- Solve the transport equation (51) to update $\phi_{n+1}(x)$;
- **if** $n \mod N_m = 0$ **then**
  - Solve the reinitialization equation (53);
  - Update $\phi_n(x) \leftarrow \psi(x)$;
- **while** $\tilde{J}_\mu(\phi_{n+1}) > \tilde{J}_\mu(\phi_n)$ **do**
  - Halve the step size: $t_n = \frac{t_n}{2}$;
- Update the domain: $\Omega_{n+1} \leftarrow \Omega_n - t_n\theta_n$;

Algorithm 2: Gradient descent method for optimization with topological derivative.

Input: Initial level-set function ϕ_0, initial step size τ_0, stopping tolerance $Tol > 0$, maximum number of iterations $n_{\max} \in \mathbb{N}$, multiplier μ.

for $n = 0, 1, 2, \ldots, n_{max}$ **do**

- Solve the state equation (7) and the adjoint state equation (17);
- Compute the generalized topological derivative $\tilde{\mathcal{T}}(\Omega_n)$;
- Set $g_n = -P_{\phi_n^\perp}\left(\tilde{\mathcal{T}}(\Omega_n)\right) = -\left(\tilde{\mathcal{T}}(\Omega_n) - \frac{(\tilde{\mathcal{T}}(\Omega_n), \phi_n)}{\|\phi_n\|^2_{L^2(D)}}\phi_n\right)$;
- Compute $\theta_n = \arccos\left(\frac{(\phi_n, \tilde{\mathcal{T}}(\Omega_n))_{L^2(D)}}{\|\psi_n\|_{L^2(D)}\|\tilde{\mathcal{T}}(\Omega_n)\|_{L^2(D)}}\right)$;
- **if** $\theta_n < Tol$ **then**
  - Stop with approximate minimizer Ω_n;
- **while** $J_\mu(\phi_n - \tau_n g_n) > J_\mu(\phi_n)$ **do**
  - Halve the step size: $\tau_n = \frac{\tau_n}{2}$;
- Update the level-set function: $\phi_{n+1} = \phi_n - \tau_n g_n$;

Algorithm 3: Combining shape gradient (gradient flow) and topological derivative for optimization.

Input: Initial level-set function ϕ_0, initial step sizes t_0 and τ_0, stopping tolerance $Tol > 0$, maximum number of iterations $n_{\max} \in \mathbb{N}$, multiplier μ.

for $n = 0, 1, 2, \ldots, n_{max}$ **do**
- Solve the state equation (7) and the adjoint state equation (17);
- **if** $n \mod m = 0$ **then**
  - Compute the topological derivative $\tilde{\mathcal{T}}(\Omega_n)$;
  - Set $g_n = -P_{\phi_n^\perp}\left(\tilde{\mathcal{T}}(\Omega_n)\right) = -\left(\tilde{\mathcal{T}}(\Omega_n) - \frac{(\tilde{\mathcal{T}}(\Omega_n), \phi_n)}{\|\phi_n\|^2_{L^2(D)}}\phi_n\right)$;
  - Update the level-set function using the topological derivative: $\phi_{n+1} = \phi_n - \tau_n g_n$;
  - **while** $J_\mu(\phi_{n+1}) > J_\mu(\phi_n)$ **do**
    - Halve the step size: $\tau_n = \frac{\tau_n}{2}$;
- **else**
  - Compute the shape gradient $\tilde{J}_\mu(\Omega_n)'$;
  - Solve the gradient flow to obtain θ_n;
- Update the domain: $\Omega_{n+1} \leftarrow \Omega_n - t_n\theta_n$;

Contents

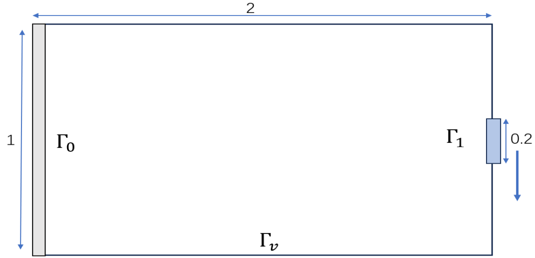

Figure: Structural model diagram

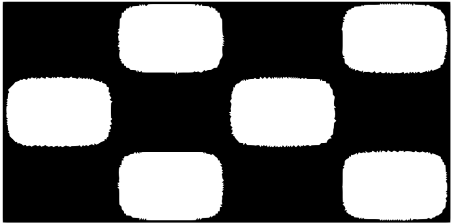
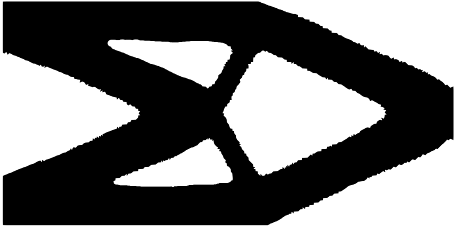

Figure: Initial domain (left) and optimized structure (right)

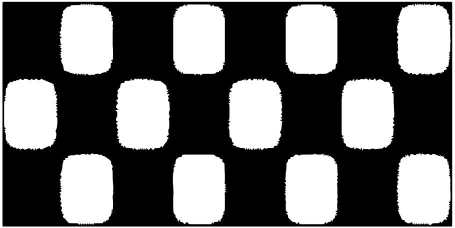


Figure: Initial domain (left) and optimized structure (right)

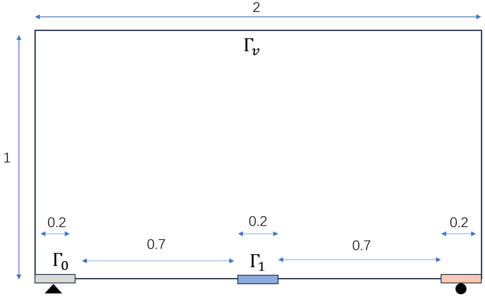

Figure: Structural model diagram

Figure: Final structures obtained with different algorithms

Other results

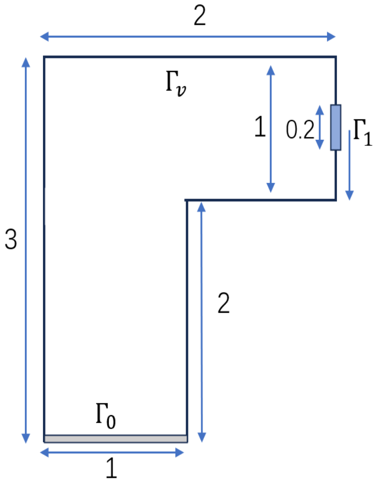

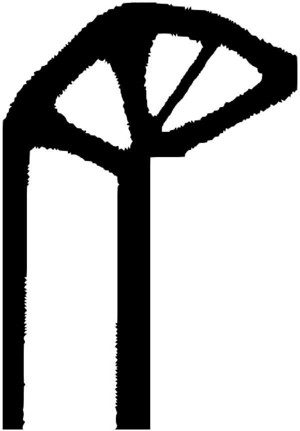

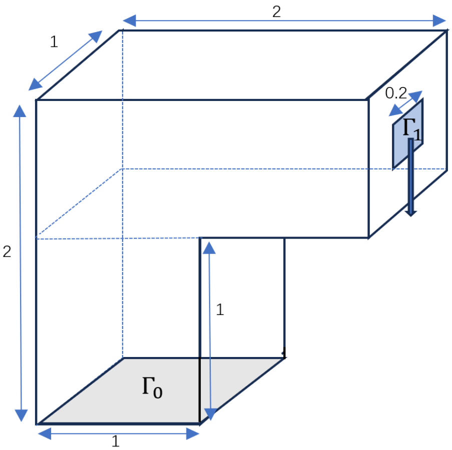
2
1
0.2
Γ_1
2
1
Γ_0
1

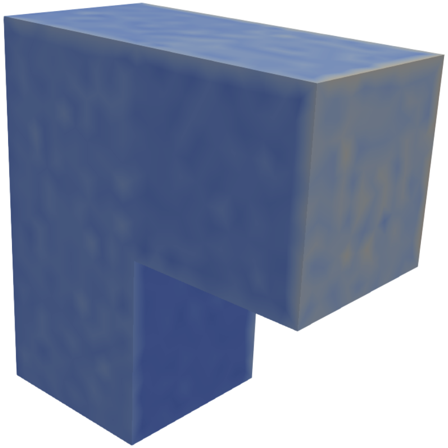

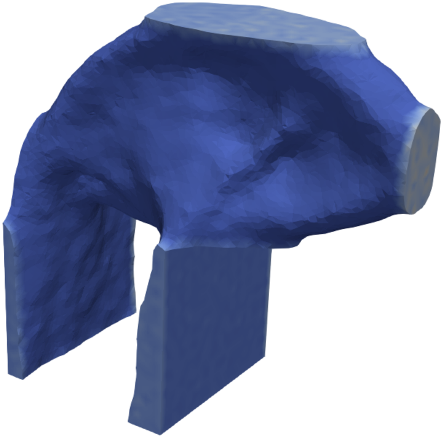

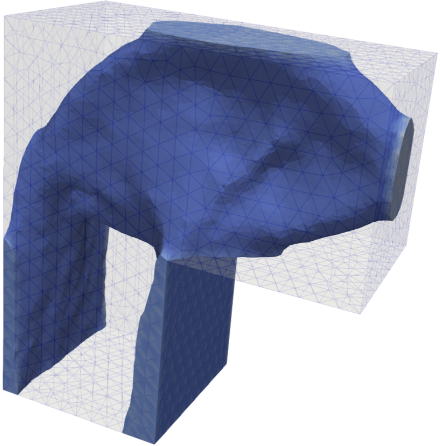

Reference

- Nowak M, Sokołowski J, Żochowski A. Biomimetic approach to compliance optimization and multiple load cases. *Journal of Optimization Theory and Applications*, 184(1):210–225, 2020.
- Nowak M, Sokołowski J, Żochowski A. Justification of a certain algorithm for shape optimization in 3D elasticity. *Structural and Multidisciplinary Optimization*, 2018, 57(2):721–734.
- Nowak M, Sokołowski J, Żochowski A, Polak J. On Compliance Minimization by Biomimetic Regularization Method[J]. Bulletin of the Polish Academy of Sciences Technical Sciences, in press. DOI:10.24425/bpasts.yyyy.xxxxxx.
- Plotnikov P. I. , Sokolowski J. Gradient Flows in Shape Optimization Theory. *Doklady Mathematics*, 108(2):387–391, 2023.

Thank you!